Atomic-scale insights into 1D and 2D nano-materials

U Bangert[1], W Pierce[2], C B Boothroyd[3], M Migliorato[4], C-T Pan[2], A J Harvey[1], D M Kepatsoglou[5], Q M Ramasse[5]

[1]Department of Physics and Energy, University of Limerick, Limerick, Ireland,
[2]School of Materials, The University of Manchester, Manchester M13 9PL, U.K.
[3]Ernst Ruska-Centre for Microscopy and Spectroscopy with Electrons and Peter Gruenberg Institute Juelich Research Centre, D-52425 Juelich, Germany
[4]School of Electrical and Electronic Engineering, The University of Manchester, Manchester M13 9PL, U.K.
[5]SuperSTEM Laboratory, STFC Daresbury Campus, Daresbury WA4 4AD, United Kingdom
e-mail: Ursel.Bangert@ul.ie

Abstract. Atomic resolution imaging and narrow-energy spread spectroscopy in aberration corrected (scanning) transmission electron microscopes, in combination with DFT modelling has made it possible to uncover atomic-scale morphology, defect constellations, lattice impurities and ad-atoms in nano-materials, as well as revealing their influence on the surrounding bandstructure. Using atomic-scale imaging, EEL spectroscopy and EFTEM, we address issues beyond the more common investigations of their atomic lattice structure. We focus on the demonstration of (i) ripples in graphene and on effects of (ii) metal ad-atoms as well as of (iii) controllably introduced impurities -via low energy ion implantation- in both, graphene and carbon nanotubes, on the electronic band structure. We demonstrate the creation of a new feature with collective charge carrier behaviour (plasmon) in the UV/vis range in graphene and carbon nanotubes via EEL spectrum imaging and EFTEM, and support this with dielectric theory modelling.

1. Introduction. Graphene and carbon nanotubes have been intensively investigated via electron microscopy methods [1-3] regarding their atomic structure, and peculiarities of the latter introduced by changes of morphology, e.g., at the edges of carbon sheets or through impurities [4,5]. Less frequently addressed phenomena concern the local topography (flatness), especially of suspended graphene, and its implications on electronic structure. The effect of impurity incorporation, albeit through physio-chemical adsorption, bonding or integration into the carbon lattice on bandstructure in the eV regime, i.e., in the UV/vis energy excitation regime is a further, less actively researched area; the research focus is predominantly on terahertz and infrared physics/ applications with regards to opto-electronics and plasmonics. Controlled impurity integration, leading to bandstructure tailoring other than by electric gauging or chemical functionalization, is a field of interest, as chemical methods have significant drawbacks due to lack of control, contamination and inferred secondary impurities, instability and site selectivity. Ion implantation, enabling flexible small-depth channel doping (like in semiconductor-technology) is a prospective method for non-chemistry reliant functionalisation and processing of 2D and 1D materials [6,7]. Here we present a selection of investigations concerning the above topics with the aim of demonstrating impact of nano-structure on electronic bandstructure phenomena in the UV/vis energy regime.

2. Experimental. *Sample preparation.* Graphene was produced via chemical vapour deposition (CVD) of CH_4 and H_2 precursor gasses on a copper foil substrate [8]. The graphene was then transferred onto Quantifoil TEM grids, using the 'wet transfer' method [9]. Freestanding graphene produced using this method was mainly monolayer, with occasional bilayer or multilayer regions. As with all graphene, residual hydrocarbon deposits were seen on the samples. Metals were deposited onto the graphene using electron-beam or thermal evaporation with an evaporation rate of 0.1 nm/s, resulting in metal deposits of 0.1 to 0.3 nm height.

Carbon nanotubes (CNTs) were doped directly with alkali and earth alkali metals (e.g. K, Na and Ba) and B via ion implantation at ~200 eV at the Surrey University Ion Beam Centre, and with B and Ag, under the same conditions, at the Salford University Low Energy Ion Implanter, all to doses of

10^{14}-10^{15} cm^{-2}. The implantation energy was chosen to ensure uniform doping over the volume of nanotubes containing multiple carbon sheets. Substitutional doping of graphene was achieved using ultra-low-energy ion implantation [6]. Energies of ~25 eV were chosen and implantation was carried out with the University of Göttingen mass selected ion beam deposition system [10, 11], directly into free standing graphene, at doses between 10^{14} and 10^{15} cm^{-2}. In support of the ultra-low energy ion-implantation experiments, simulations of the implantation process in graphene were previously performed in Göttingen using the Monte Carlo program SDTrimSP [10,12], suggesting doping levels of 1.5 to 5 at% [6, 10]. Previous HRTEM investigations indicate nitrogen doping levels ranging from 0.1 at% to 1 at% [6], and higher (few %) for alkali-ions in CNTs.

Data acquisition. Energy filtered TEM (EFTEM) imaging and energy loss spectroscopy (EELS) in conjunction with high resolution bright field microscopy (HREM) were carried out at the Ernst-Ruska Centre, Jülich, on an FEI Titan 50-300 Pico triple aberration corrected and monochromated TEM operated at 80 keV. The microscope is equipped with a Gatan UltraScan 4000 UHS CCD with 4k x 4k pixels. EFTEM images and EELS were acquired using a Gatan Quantum ERS image filter with fully 2nd and 3rd order and partially 4th order corrected prisms. EFTEM images were acquired with a slit width of between 0.4 and 1 eV and with energy step sizes of between 0.1 eV and 0.5 eV. EEL spectra were (i) extracted from EFTEM data cubes or (ii) directly acquired in scanning (STEM) mode. Monochromation of the electron beam enabled the FWHM of the zero-loss peak to be reduced to around 0.1 eV. Additionally, atomic resolution HAADF and Spectrum imaging were carried out on the Daresbury Nion UltraSTEM, with a spectrum resolution of 0.3 eV. Graphene HREM images were additionally obtained in the Warwick ARM 200F.

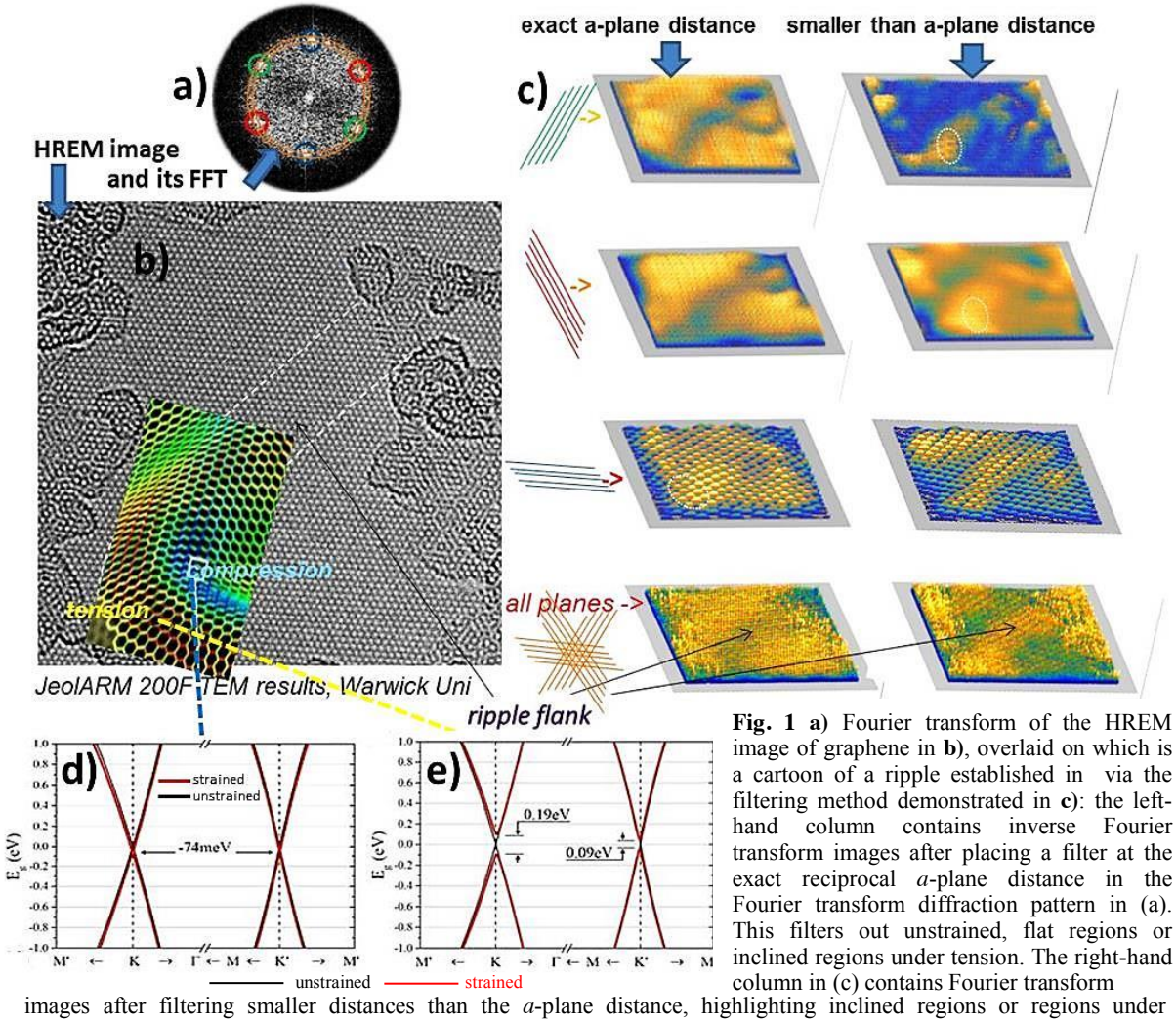

Fig. 1 a) Fourier transform of the HREM image of graphene in **b)**, overlaid on which is a cartoon of a ripple established in via the filtering method demonstrated in **c)**: the left-hand column contains inverse Fourier transform images after placing a filter at the exact reciprocal *a*-plane distance in the Fourier transform diffraction pattern in (a). This filters out unstrained, flat regions or inclined regions under tension. The right-hand column in (c) contains Fourier transform images after filtering smaller distances than the *a*-plane distance, highlighting inclined regions or regions under compression; **d)** bandstructure at the Dirac points, calculated by tight binding, predicting a bandgap of 0.19 eV at the K point of the Brillouin zone in regions of tensile strain; **e)** no bandgap opening occurring in regions of compressive or low (to zero) strain. However for compressive strain the Dirac point lies below the Fermi energy by 74meV.

Data evaluation. Zero-loss peak (ZLP) extraction was carried out in Gatan Digital Micrograph (DM) by fitting a power-law background to the ZLP using a vacuum spectrum (obtained far from the sample) as a guide. An alternative approach, using the reflected-tail function in DM, was used for the EFTEM images recorded on the monochromated Titan Pico, with the monochromation achieving small and nearly symmetric tails of the ZLP. In some cases (on spectra obtained from metal- and B-doped CNTs) Richardson Lucy (RL) deconvolution was applied, bringing the spectral information down to 1 eV.

Calculations and modelling of low loss EEL spectra entailed calculations of the energy loss function and complex dielectric function of graphene and SWNT systems using the WIEN2K DFT code [13], aiding investigations of whether an excitation is of collective (plasmon) nature. The dielectric function was also extracted from experimental EEL spectra using the Kramers-Kroenig Analysis programme in Digital Micrograph (with a refractive index of around 2; a full description of the analysis method can be found in the Gatan Documentation, EELS Analysis, Copyright 2012 Gatan Inc.).

3. Results and Discussion.

(i) *Ripples*. Contamination-free areas in suspended graphene are not atomically flat, but have been shown to have static ripples [14,15], of the order of up to 10 nm in width and a couple of nm in height. Apart from direct observation via STEM [15] the morphology of ripples can be obtained via Fourier filtering of atomic resolution lattice images [14]. Figure 1a) shows an FFT of the area shown in fig.1b. A spot filter mask was then set to encompass regions around the diffraction spots at different reciprocal distances. Figure 1c (left-hand column) shows inverse FFT images after having set a spot mask at the exact *a*-plane distance (concentrically encompassing the diffraction spots) for the three *a*-planes in turn. The inverse FFT will then filter out exact *a*-plane distances/ bond lengths in flat regions, as well as bonds, which are longer (tension), but on inclined surfaces, resulting in a projected bond length that appears the same as that of the graphitic *a*-planes. Figure 1c (right-hand column)

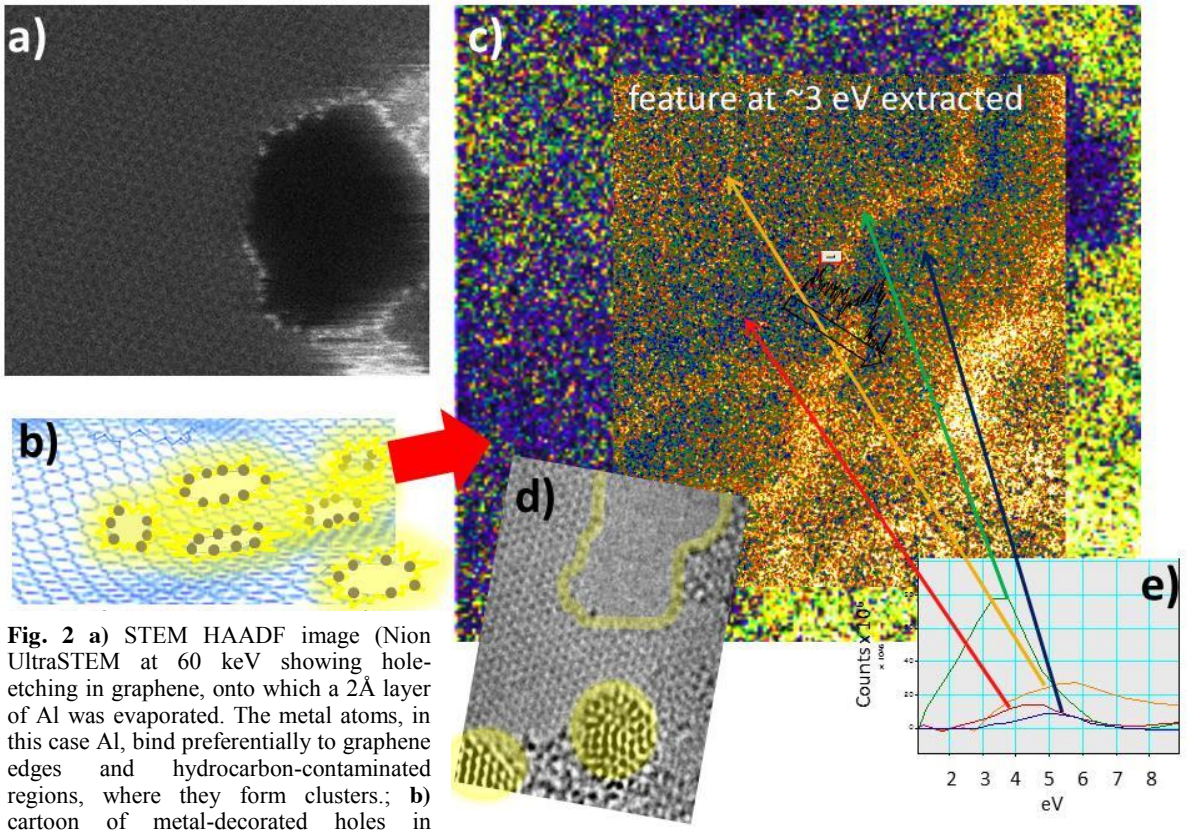

Fig. 2 a) STEM HAADF image (Nion UltraSTEM at 60 keV showing hole-etching in graphene, onto which a 2Å layer of Al was evaporated. The metal atoms, in this case Al, bind preferentially to graphene edges and hydrocarbon-contaminated regions, where they form clusters.; **b)** cartoon of metal-decorated holes in graphene, giving rise to enhanced plasmon emission, as experimentally observed; **c)** ZLP subtracted EFTEM image (blue and yellow colours) with overlaid EFTEM image after ZPL and π-plasmon subtraction (orange and blue colours) at the excitation energy of 3-4 eV, of Pd-dosed graphene, showing enhancement in the UV/vis regime at the graphene edge around a hole. An intensity profile along the black arrow across the hole's edge shows ~50% enhancement. The very bright intensity at the bottom of the EFTEM image stems from Pd crystals; **d)** overlaid structural (HREM) image, with dark dots overglossed by yellow sheen) representing Pd atoms; **e)** intensity of residual EEL signal after removal of the excitation in the π-plasmon region at 4.5 eV, revealing the new plasmon feature at slightly above 3 eV, only visible in the presences of Pd-atom decoration (frame width of EFTEM images ~15 nm).

shows inverse FFT images after setting a spot mask at a reciprocal distance a fractional % larger than the *a*-plane distance. The inverse FFT will then filter out *a*-plane distances/ bond lengths in flat regions that are smaller than the graphene *a*-plane distance (compression) as well as *a*-plane bonds on inclined surfaces, whose projected bond lengths therefore appear shorter than those of the graphitic *a*-planes in 'flat projection'. The colour coding (temperature scale) in figure 1c reveals a ripple crossing the image area diagonally, as indicated by the overlaid cartoon in fig. 1b. The band structure of rippled graphene was then calculated by tight binding (colours in the cartoon indicate extended/tensile (red) or compressed (blue) bonds). The bandstructure at the Dirac points in fig. 1e predicts a bandgap of 0.19 eV at the K point of the Brillouin zone in the regions of tensile strain. Regions of compressive or low (to zero) strain (green) in the cartoon do not exhibit a bandgap. However for compressive strain (fig. 1d) the Dirac point lies below the Fermi energy by 0.074eV.

(ii) *Nano-sculpting*. Following previous observations by the authors of hole formation after metal-evaporation on graphene, via metal-mediated etching in the presence of oxygen [16], and decoration of these holes with metal atoms [17,18] (see fig. 2a), we here go on studying the effects of metal-decorated holes on excitations in the UV/vis for the case of Pd. Rather than evenly covering the graphene, Pd (as all metals) forms nanoparticles of few nm in diameter (fig. 2d, dark-dot clusters with yellow sheen). In line with previous studies of the metal-graphene interaction [17], all nanoparticles sit on contamination and do not reside on pristine graphene surfaces; neither have single Pd-atoms been detected on clean graphene patches. In explanation of this, theoretical works have predicted very low binding energies for metals on monolayer graphene [19]. Figure 2c shows an EFTEM image of an excitation energy window at 3-4 eV, extracted from a data cube acquired from 17.5 eV to -2.5 eV in reverse mode, from high to low energy, to avoid afterglow effects from the high-intensity low loss region with an energy selecting slit width of 1 eV, an energy step size of 0.5 eV and an exposure time of the extracted slice of 5 seconds. Enhancement of the excitation at ~3 eV can be seen around two holes in the graphene, which are decorated by individual Pd-atoms, seen as dark dots in fig. 2d). The very bright yellow regions (the intensity is displayed on the temperature scale) arise from surface plasmons in Pd nanoparticles. In order to obtain the energy filtered image overlaid in the middle of fig. 2c (orange/blue colours) the excitation in the π-plasmon region at 4.5 eV was assimilated by a Gaussian peak, providing a simple and very good fit to the experimental data, and subtracted from the data cube (from which so far only the ZLP had been subtracted; blue/yellow colours in large underlying image 2c). The enhancement is spatially confined to less than 0.5 nm along the edge of the hole. Line profiles of the integrated loss intensity in the 3-4 V energy regime across edges of holes (one such scan location is shown as black arrow in fig. 2c together with the corresponding intensity profile) show a relative enhancement over that of pristine graphene of up to 50%. Example spectra extracted from EFTEM cubes together with arrows pointing to the respective locations, are shown in fig. 2e. The excitation at ~3 eV is clearly largest at the hole's edge. It has been disputed whether excitations at these energies are plasmons. The criterion for a Drude plasmon is a negative-to-positive zero-crossing of the real part of the dielectric function at the plasmon

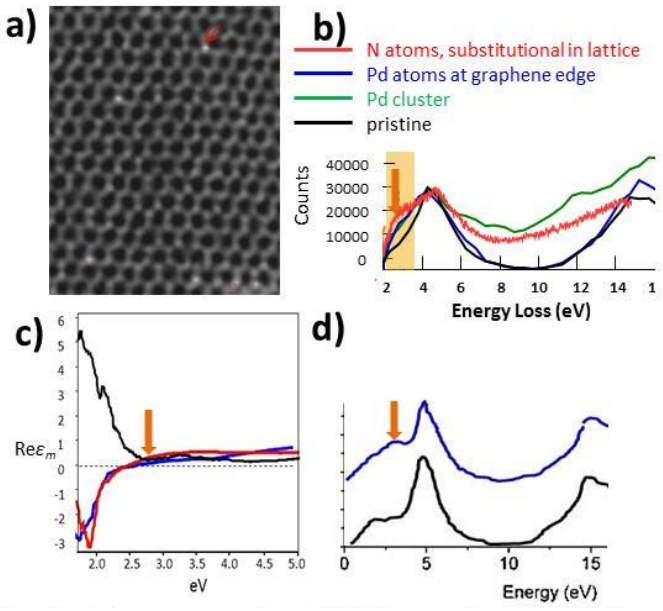

Fig. 3 a) Atomic resolution HAADF image (Nion UltraSTEM) of N-implanted graphene showing substitutional N atoms as bright dots (e.g., red arrow); **b)** experimental low-loss spectra extracted from EFTEM data cubes (TitanPICO); **c)** real part of the dielectric function extracted via Kramers-Kroenig analysis from the spectra in (b), of N-implanted, pristine and Pd-decorated hole-edges in graphene; **d)** simulated in-plane EEL spectra of a single Pd adatom on graphene in a 4x4 supercell, and of pristine graphene. The orange arrows point to the new feature at 3-3.5 eV in the experimental as well as the modelled spectra; it also denotes the zero-crossing in the dielectric function, indicating the plasmonic nature of this feature.

energy. A zero-crossing for spectra exhibiting the 3-eV feature can be seen in fig. 3c; it reveals that this feature is of plasmonic nature.

(iii) *Controlled impurity incorporation*. We have previously demonstrated that, in contrast to chemical doping or dosing via physi-sorption, it is possible to directly integrate metals, N and B into the lattice of graphene and CNTs via low-energy ion implantation [6,7] (see fig. 3a, and figs 4a&c). Figure 3b shows that, similar to Pd-dosing, N-doping introduces an excitation at ~3 eV in graphene, which is of plasmonic nature, as revealed by the zero-crossing of the dielectric function (fig. 3c).

Ion implantation of CNTs with Ag results in intercalation (fig. 4a) and a strong excitation at 3eV (fig. 4b). Out of the alkali metals, only K showed clear results, namely in in-plane doping (fig. 4c) and a plasmonic excitation at ~3 eV (fig. 4c, d & e). B doping also leads to lattice integration in both,

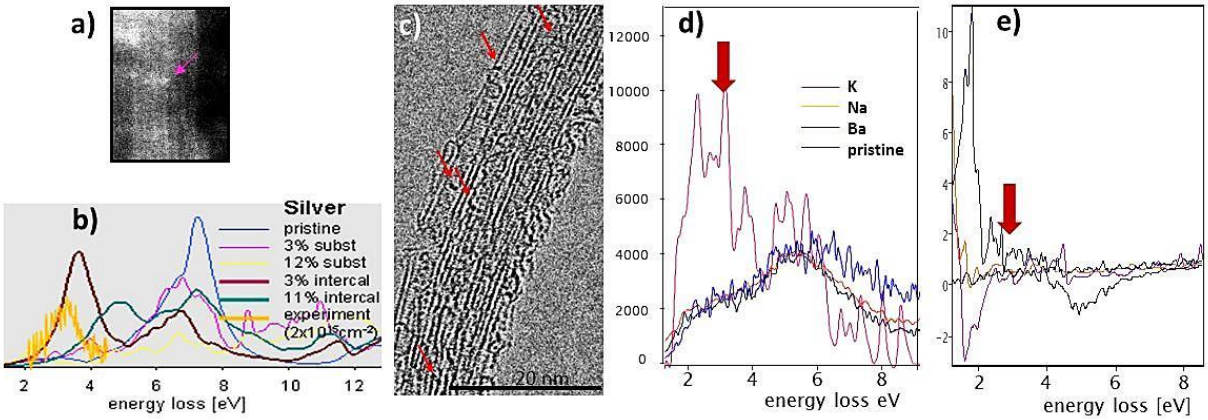

Fig. 4 a) Atomic resolution HAADF) image (Nion UltraSTEM) of an Ag-implanted MWCNT at 200 eV to a dose of 2x10^{15} cm^{-2}, revealing intercalated Ag-atoms (purple arrow); **b)** calculated (DFT: WIEN2K) low loss EEL spectra of MWCNTs with Ag-dopants in substitutional and intercalated positions, as well as experimental loss EEL spectrum of the tube in (a); **c)**) HREM image (TitanPICO) of K-doped DWNT bundle; dark dots (some are arrowed) are K-atoms integrated into the graphene sheets; **d)** low loss EEL spectra of DWNTs and SWNT bundles implanted with alkali and earth-alkali metals (TitanPICO). The spectrum intensity is normalised to the feature at ~5 eV (pi-plasmon). Doping with the metals was achieved by ion implantation at 200 eV to a dose of 10^{15} cm^{-2}; **e)** Reε_m of the dielectric function extracted via Kraemers-Kroenig analyisis from the experimental spectra (smoothed with a low pass filter with w= 0.2 eV).

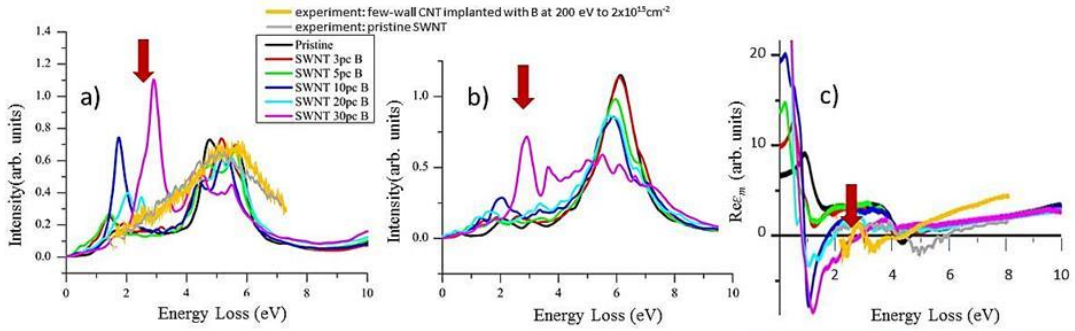

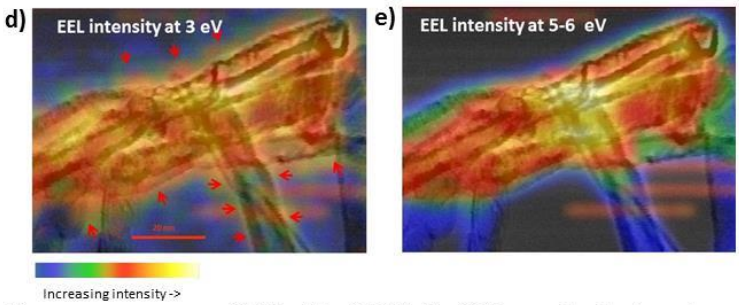

Fig. 5 a) Calculated electron energy loss spectra (DFT: WIEN2K) of a (substitutionally) boron doped (10,10) SWNT bundle in the out-of-plane and **b)** the in-plane direction, **c)** calculated out-of-plane component of the real part of the dielectric function. Also overlaid in (a) and (c) are experimental spectra of a heavily B-doped and a pristine carbon nanotube; **d)** background subtracted EEL map of an aggregate of double- and few-layer CNTs at 2-3.5eV and **e)** at 4.7-6.5 eV extracted from an SI (NionUltraSTEM). The CNTs were ion-implanted at an energy of 200 eV, to a dose of 2x10^{15} cm^{-2}. The EEL map is overlaid on the Bright Field STEM image of the tubes (black shapes). Arrows in the left-hand image mark positions that indicate that the lower energy signal is less localised than the π-bulk plasmon (right) and more concentrated on the surface of the tubes; relatively higher intensity is seen here in the vacuum.

4. Conclusion. We have demonstrated the existence of ripples in graphene, which, according to calculations could shift the Dirac point and introduce a bandgap. Metal deposition on graphene leads to formation of metal ad-atoms decorating the holes, with creation/enhancement of a plasmonic feature at UV/vis energies along their edges. A similar feature is introduced by ion-implantation of N into graphene with N on substitutional sites, and of K and B into carbon nanotubes, with both species integrated into the carbon lattice. Ion implantation of Ag leads to intercalation, resulting in a similar excitation. It appears that heavier metals intercalate, whereas K, N and B integrate into the carbon lattice. All these impurities create a plasmon feature at around 3 eV.

Acknowledgements. We thank R. Gwilliam at the University of Surrey and J. Van den Berg at the University of Salford as well as their teams for ion-implantations into CNTs, and H. Hofsaess and J. Amani from the Universitaet Goettingen for ion implantations into graphene and CNTs. We are also indebted to R. Zan for preparation of graphene TEM samples at the University of Manchester and to R. J. Kashtiban from Warwick University for providing HREM images of graphene.

References.

[1] Banhart F, Kotakoski J and Krasheninnikov A V 2011 *ACS Nano* **5** 26
[2] Meyer J C , Kisielowski C, Erni R, Rossell M D, Crommie M F and Zettl A 2008 *Nano Lett*. **8 (11)** 2582
[3] Gass M H, Bangert U, Bleloch A L, Wang P, Nair R L R and Geim A K 2008 *Nat*. *Nano*. **3** 676
[4] Wang H, Wang Q, Cheng Y, Li K, Yingbang Y, Zhang Q, Dong C, Wang P, Schwingenschlögl U, Yang W and Zhang X X 2012 *Nano Lett*. **12** 141
[5] Bangert U and Zan R 2015 *Int*. *Mat*. *Rev*. **60(3)** 133
[6] Bangert U, Pierce W, Kepaptsoglou D M, Ramasse Q M, Zan R, Gass M H, Van den Berg J A, Boothroyd C B, Amani J and Hofsäss H C 2013 *Nano Lett*. **13 (10)** 4902
[7] Bangert U, Bleloch A, Gass M H, Seepujak A and Van den Berg J A 2010 *Phys Rev B* **81** 245423
[8] Li X, Cai W, An J, Kim S, Nah J, Yang D, Piner R, Velamakanni A, Jung I, Tutuc E, Banerjee S K, Colombo L and Ruoff R S 2009 *Science* **324** 1312
[9] Reina A, Son H, Jiao L, Fan B, Dresselhaus M S, Liu Z and Kong J, 2008 *J*. *Phys*. *Chem*. *C* **112** 17741
[10] XuY, Zhang K, Brusewitz C, Wu X and Hofsäss H C 2013 *AIP Advances* **3** 072120
[11] Hofsäss H, Ronning C and Feldermann H 2001 *Proc. 16th Int Conf on the Application of Accelerators in Research and Industry, Denton, TX, USA*, Nov 1-4 2000, eds. Jerome L Duggan and I Lon Morgan *AIP Conf. Proc.* ***576*** 947
[12] Eckstein W, Dohmen R, Mutzke A and Schneider R "SDTrimSP: A montecarlo code for calculating collision phenomena in randomized targets" 2007
[13] Blaha P, Schwarz K, Madsen G K H, Kvasnicka D and Luitz J 2001 *Wien2k User's Guide* http://www.wien2k.at/reguser/textbooks
[14] Bangert U, Gass M H, Bleloch A L, Nair R R and Geim A K 2009 *phys stat sol a* doi:10.1002/pssa.200824453
[15] Zan R, Muryn C A, Bangert U, Mattocks P, Wincott P,Vaughan D, Ruoff R S, Hamilton B and Novoselov K S 2012 *Nanoscale* **4** 3065
[16] Ramasse Q M, Zan R, Bangert U, Boukhvalov D W, Son Y-W and Novoselov K S 2012 *ACS Nano* **6 (5)** 4063
[17] Zan R, Bangert U, Ramasse Q M, Novoselov and K S 2011 *Nano Letters* **11(3)** 1087
[18] Zan R, Bangert U, Ramasse Q M and Novoselov K S 2012 invited Perspective *J*. *of Phys*.*Chem*. *Lett*. **3 (7)** 953
[19] Hardcastle T P, Seabourne C R, Zan R, Brydson R M D, Bangert U, Ramasse Q M, Novoselov K S and Scott A J 2013 *Phys*. *Rev*. *B* **87** 195430.